Performance of the H9 Magnetically Shielded Hall Thrusters

IEPC-2017-239

Presented at the 35th International Electric Propulsion Conference
Georgia Institute of Technology – Atlanta, Georgia – USA
October 8–12, 2017

Sarah E. Cusson,*
University of Michigan, Ann Arbor, MI 48109

Richard R. Hofer,† Robert Lobbia ‡
Jet Propulsion Laboratory, California Institute of Technology, Pasadena, California, 91109

and

Benjamin A. Jorns,§ and Alec D. Gallimore¶
University of Michigan, Ann Arbor, MI 48109

The results from the acceptance and performance tests of three laboratory-model, 9-kW, magnetically-shielded Hall thrusters are presented. These thrusters, built through a joint development program led by the Jet Propulsion Laboratory in collaboration with the University of Michigan and the Air Force Research Laboratory, are intended to serve as standardized testbeds for investigating the relatively new technology of magnetic shielding. Acceptance testing consisted of flow uniformity measurements of the anodes, mapping of the magnetic field topography in each thruster, and far field measurements of the symmetry of the thruster plumes. All models were found to be within the acceptance criterion of 10% total deviation from the average. The stability of the thrusters, as quantified by oscillations in the discharge current, also was investigated. It was found that all three thrusters exhibited discharge current oscillations less than 80% of the mean current over the design range of magnetic field magnitude and operating conditions. The performance of one thruster was characterized over the designed throttling range: operating powers from 4.5 to 9 kW and discharge voltages ranging from 300 to 800 V. The measured thrust extended from 291 mN to 436 mN, with a maximum total efficiency of 63.4%, and a maximum specific impulse of 2950 seconds. All three thrusters ultimately passed the acceptance criteria and are now being used in active research campaigns at multiple United States institutions.

*Ph.D Candidate, Department of Aerospace Engineering, cusson@umich.edu
†Supervisor, Electric Propulsion Group
‡Staff Engineer, Electric Propulsion Group, formerly with the Air Force Research Laboratory, ERC Inc., Edwards AFB, CA
§Assistant Professor, Department of Aerospace Engineering
¶Robert J. Vlasic Dean of Engineering, the Richard F. and Eleanor A. Towner Professor of Engineering, and Arthur F. Thurnau Professor of Aerospace Engineering

Nomenclature

$\frac{B}{B_o}$	= relative magnetic field strength
g	= gravitational constant
I_d	= discharge current
I_{sp}	= specific impulse
$\dot{m}$	= mass flow rate
P	= power
$\bar{P}$	= mean pressure
r	= radial position
R_m	= mean channel radius
T	= thrust
V_d	= discharge voltage
δP_{max}	= maximum deviation in pressure from the mean
η	= efficiency

I. Introduction

The erosion of the discharge chamber has historically been the major life limiting factor of Hall effect thrusters. With the implementation of magnetic shielding technology, however, this wear mechanism largely has been eliminated.[1,2] Indeed, recent experimental campaigns have shown that erosion rates of the channel walls in a magnetically shielded Hall thruster can be up to three orders of magnitude lower than the erosion rates exhibited by comparable, un-shielded thrusters.[2]

The physics of magnetic shielding emerged from a combination of empirical observation and numerical investigation. During a duration wear test of the XR-5 by Aerojet Rocketdyne, it was noted that after 5600 hours of the 10000 hour test, the erosion of the thruster walls began to asymptote to a zero-erosion state.[3] A subsequent numerical investigation headed by the Jet Propulsion Laboratory uncovered the underlying physics that resulted in this low-erosion state.[4] These insights led to guiding principles for designing thrusters with magnetically-shielded walls that would not exhibit erosion—even at the beginning of life.[3–5] The physics of magnetic shielding subsequently was validated in a series of tests on the H6MS, a 6-kW thruster, based on the H6 design and retrofitted to be magnetically shielded.[1,2]

The successful demonstration of magnetic shielding from first-principles has many mission-enabling implications. Indeed, it is now believed to be possible to extend the life of Hall thrusters by at least an order of magnitude over state of the art. This in turn has led to the base-lining of the magnetic shielding technology on the HERMeS thruster, as well as the consideration for shielded thrusters on other missions. Despite the promise of shielding, however, it is still a relatively new technology and there are open questions about its operation and potential implications. For example, the oscillations in these devices appear to have different character[6] and there also is slight but anomalous pole erosion in these devices not seen in unshielded counterparts. Moreover, in comparison to more traditional unshielded thrusters, there is only a small body of data available on the internal plasma properties in these devices as well as the effects of external factors such as facility interactions on thruster operation. With these open and pressing questions in mind, the need is an apparent for additional research programs devoted to shielded thrusters. Moreover, to facilitate these efforts and enable direct comparison with results from multiple parallel programs, there is a strong argument for developing a standardized, magnetically-shielded test article that could be evaluated at multiple US institutions.

With the goal in mind, the ideal test article would be capable of operating at the high-specific impulses (up to 3000 seconds) and efficiencies (greater than 60%) that are now considered state of the art for Hall thrusters while still being capable of being tested below 20 μTorr without requiring prohibitively large pumping capability. The system similarly should have a mechanical design capable of easily incorporating various plasma diagnostics and potential hardware changes. The H6MS is a possible candidate for such a test bed. However, since it was a retrofit of an unshielded model, it has inherent limitations[2] on the magnitude and shape of the magnetic topography that can be achieved. On the other hand, while NASA used magnetic shielding in developing the 12.5 kW HERMeS thruster,[7,8] this system is a flight development unit operating at power levels that can exceed the capabilities of many research institutions.[9] Faced with these limitations for the use of current systems as a template for the test bed, the Jet Propulsion Laboratory (JPL), in collaboration with the University of Michigan (UM) and the Air Force Research Laboratory (AFRL), has developed a new, laboratory-model 9 kW Hall thruster with magnetic shielding.[9] The new thruster, the H9MS or simply H9, leverages design heritage from the H6MS: mainly the channel dimensions. However, it is without the same constraints on magnetic field margin as the H6MS. Consequently, the improved magnetic circuit allows full-shielding to occur at high discharge voltages, enabling long-life operation at 800 V, 9 kW.

While our companion paper[9] outlines the design of the H9, we present here an overview of the acceptance and performance testing of three separate units that were fabricated: one each for JPL, UM, and AFRL. To this end, we first show acceptance testing results for all three units including a description of the anode flow uniformity testing as well as the magnetic field verification. Second, we present measurements from performance testing conducted at UM including initial firing results, stability mapping, and far-field Faraday probe sweeps. We finally show performance measurements from a campaign conducted on the test article built for JPL. Since the H9 design heavily leverages heritage from the H6MS, we use this thruster's performance as a baseline when evaluating our measurements of the H9.

II. Test Equipment

A. H9 Hall Thruster

(a) (b)

Figure 1: (a) One of the H9 Hall thruster after manufacturing and (b) the H9 SN03 firing at 800 V, 9 kW during performance testing at JPL.

We manufactured three H9 Hall thrusters (Fig. 1) that are herein referred to as serial numbers (SN) 01, 02, and 03. The institutions that received SN01, SN02, and SN03 are AFRL, UM, and JPL respectively. As discussed in more detail in our companion paper,[9] each thruster features a magnetic lens topography with magnetic shielding to increase thruster lifetime. The electron sources are provided by centrally mounted lanthanum hexaboride hollow cathodes that are identical in design to those built for the H6 Hall thruster.[10] The thrusters have a nominal throttling curve from 4.5 to 9 kW and voltage range from 300 to 800 V, but can operate outside of this range. Each thruster features replaceable boron nitride rings for the discharge chamber, graphite pole covers and a stand that acts as a radiator. While the H9 thruster body is capable of operating in multiple electrical configurations, the default we employed for our acceptance testing was the cathode-tied configuration during all testing, i.e. with the cathode common electrically connected to the thruster body.[11–13]

B. Facilities

Driven in part by schedule constraints, we divided the acceptance and performance testing of the H9 between two facilities: the Large Vacuum Test Facility at the University of Michigan and the Owen's Chamber at the Jet Propulsion Laboratory.

1. Large Vacuum Test Facility

Initial testing was performed in the Large Vacuum Test Facility (LVTF) at the University of Michigan (Fig. 2). LVTF is 6 meters in diameter and 9 meter long and has previously been used to test Hall thrusters at power levels up to 60 kW.[14,15] The chamber has seven cryogenic pumps with a pumping speed of 240,000 L-Xe/s to achieve vacuum during operation. During thruster testing, the H9 discharge current was supplied by a commercially available 100 kW power supply. Four commercially available power supplies were used to power the cathode heater, keeper and electromagnets. The thruster operated on research grade xenon regulated by two commercially available mass flow controllers. A series 370 Stabil Ion Gauge was used to monitor the pressure inside the LVTF during the experiments. The gauge, seen in Figure 2, was placed approximately one meter from the thruster in line with the exit plane as suggested in Ref 16. The entrance was covered in a copper mesh grid to prevent ambient plasma from entering the gauge. The base pressure during the tests was 7×10^{-7} Torr-N_2.

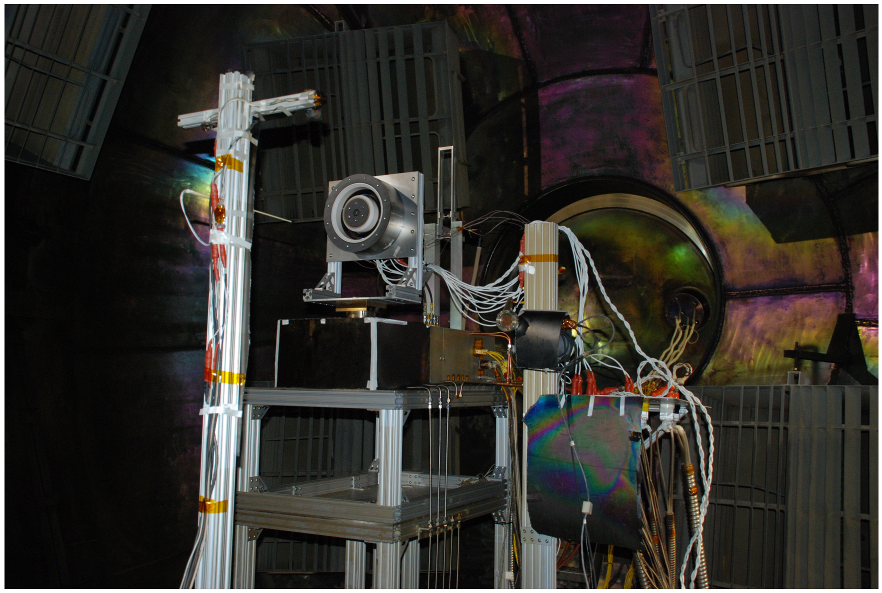

Figure 2: The H9 Hall thruster installed in the Large Vacuum Test Facility at the University of Michigan for initial testing. The probe arm with the Faraday probes can be seen in the foreground.

2. Owen's Chamber

Thrust measurements on SN03 were performed in the Owens Chamber at JPL (Figure 3). The Owens chamber is a 3 meters x 10 meters cryogenically-pumped vacuum facility. This facility has been used previously to test gridded ion and Hall thrusters at power levels exceeding 20 kW.[16–19] We monitored pressure in the Owens with a pair of ionization gauges. The first ionization gauge, used to measure the best pressure of the facility, was calibrated for nitrogen and mounted to the chamber wall downstream of the thruster exit plane. The base pressure during the tests was 9.9×10^{-7} Torr-N_2. The second ionization gauge was calibrated for xenon, mounted at the thruster exit plane and used to measured operational pressure.

Figure 3: The H9 SN03 installed in the Owen's Chamber at the Jet Propulsion Laboratory for thrust measurement testing.

C. Diagnostics

1. Thrust Stand (JPL)

We employed a water-cooled inverted-pendulum thrust stand at JPL (Fig. 3) to make thrust measurements.[20] The thrust stand operated in displacement mode with active inclination control and damping. The thruster was run through a 4 hour outgassing and warming procedure (up to 800 V) prior to any measurements being acquired. The thruster was run at a constant power for 20 to 30 minutes during which the inclination was controlled to a dead band for thrust measurements. Thermal drift and inclination of the thrust stand were accounted for during post-processing. No corrections were made for the effects of neutral ingestion due to the backpressure that ranged from 10.4-13.5 utorr-Xe. Prior testing on the H6MS has shown that the thrust is nearly invariant with backpressure and that the flow rate correction to vacuum from these pressures is about 1%.[21] Calibrations were performed by deploying a series of known weights. When inclination and thermal drift were accounted for, the response of the thrust stand was repeatable and linear to the applied force. Analysis of thrust stand data indicated an uncertainty of 1%.

2. Far-field Faraday Probe (UM)

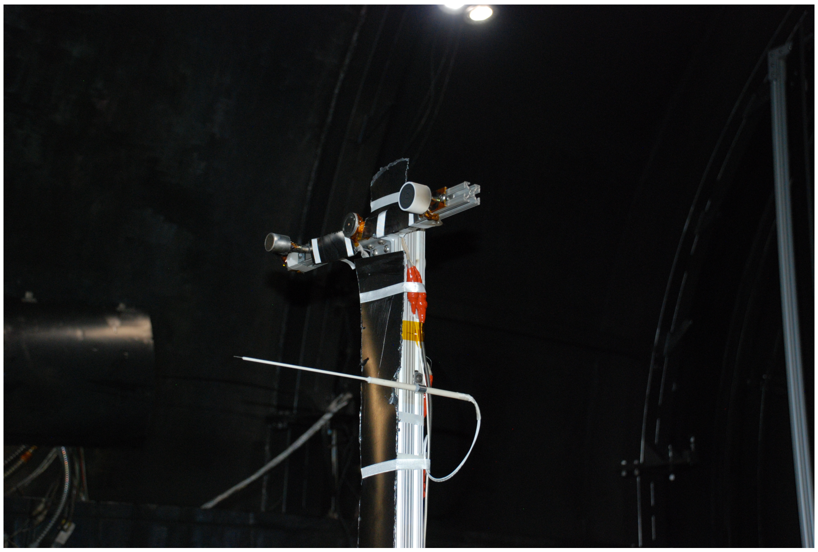

Figure 4: The three Faraday probes installed on the probe arm at the University of Michigan

Far-field Faraday probes were used to assess the uniformity and shape of the plume of each thruster at the University of Michigan. Two probes were installed in the chamber: one single collector Faraday probe and one double collector Faraday probe[22] (Fig. 4). The probe in the center (Probe 1) featured a 19.4 mm collected with a 1.4 mm gap and a 22.2 mm inner diameter guard ring. The probe on the right (Probe 2) featured an inner collector with outer diameter of 6.1 mm, a middle collector with inner diameter of 7.1 mm and outer diameter of 18.9 mm, and a guard ring with inner diameter of 20.3 mm and outer diameter of 29.9 mm. Probe 1 was intended for nominal use during all experiments and the other probe was a backup. After testing of the first thruster, Probe 1 failed, and thus we switched to the inner collector of Probe 2 for the remainder of the testing. To ensure ion saturation, the probes and guard rings were all biased to -20 V during operation. Current was measured using a Keithley Series 2400 Sourcemeter. The probes were 6.3 mean diameters downstream of the thruster and were swept at a constant axial distance back and forth across the thruster face.

III. Acceptance Testing

In addition to standard part and tolerance inspections upon assembly, we performed two additional acceptance tests on the three assembled units: an anode flow uniformity check and magnetic field mapping.

A. Anode Flow Uniformity

The azimuthal flow uniformity was assessed by neutral density testing with a Series 370 Stabil Ion Gauge at JPL (Fig. 5) The H9 discharge chamber and anodes were placed on a rotary stage with the gauge inlet located radially on channel centerline and axially midway through the discharge chamber. Each anode was measured at 36 evenly-space radial locations. We performed tests at xenon flow rates of 2 mg/s and 20 mg/s. The dwell time at each test point was 10 seconds. An acceptable flow uniformity criteria of deviations up to 10% (δP_{max}) from the mean value ($\bar{P}$) was used during testing.[23] Results, seen in Figure 6, show that all anodes were within the acceptable criteria for uniformity.

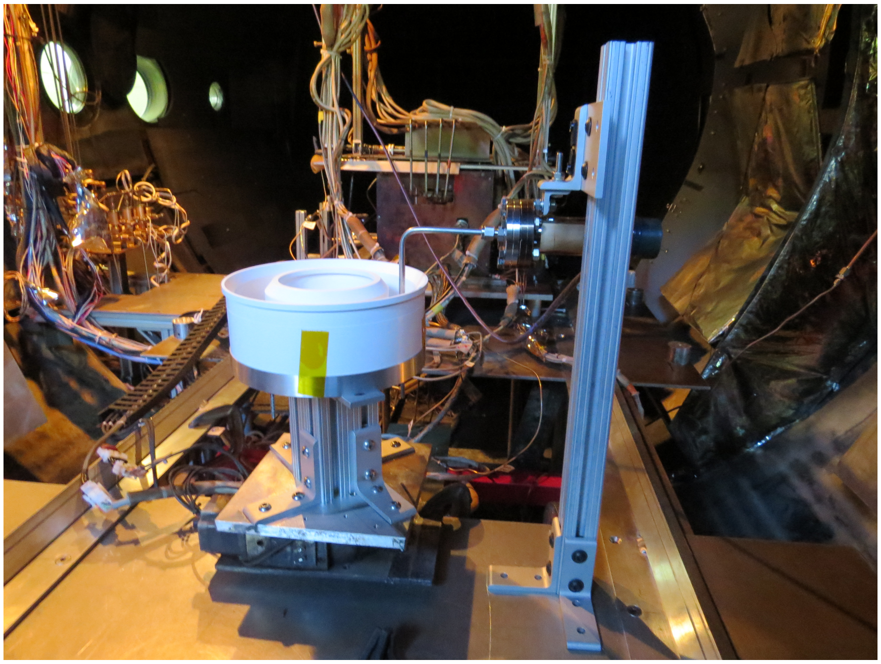

Figure 5: Test setup for anode flow uniformity testing at JPL.

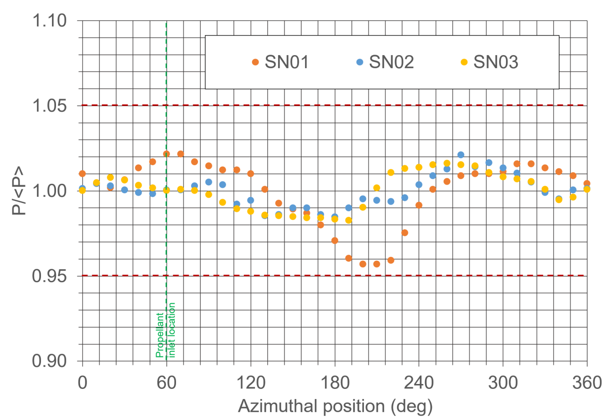

(a)

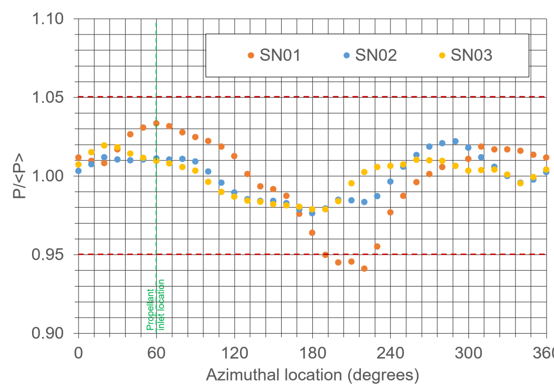

(b)

Figure 6: Flow uniformity testing results for all anodes (a) high flow testing showing all anodes within the allowable ±5% range and (b) low flow testing showing only SN01 with deviations greater than 5% from the mean. However, for SN01 the total $\frac{\delta P_{max}}{P} \times 100\%$ was still less than 10%.

During low flow testing (2 mg/s), the highest deviation minus lowest deviation with respect to the mean pressure ($\frac{\delta P_{max}}{P} \times 100\%$) was 9.23% for SN01, 4.57% for SN02, and 4.05% for SN03. As our acceptance criterion allows for a maximum allowable deviation of 10%, the three anodes thus all passed the acceptance test at this flow condition. During high flow testing, the same metric was 6.46%, 3.64%, and 3.35% for SN01, SN02, and SN03 respectively. Based on these data, all anodes similarly passed the acceptance test at the high-flow condition.

B. Magnetic Field Testing

In order to verify that the magnetic circuit was constructed properly, we mapped each thruster's magnetic field with a translating Gauss probe and compared the measurements between thrusters as well as to a reference design field shape. This latter field was originally specified during the design phase when the thruster's circuit was modeled with Infolytica's MagNet v7.5. The mapping revealed that each thruster matched the simulation and each of the other thruster's very well. In addition to two-dimensional maps, we also measured the maximum centerline radial magnetic field for each thruster. Figure 7 shows the results of this test versus inner coil current. Figure 7a shows that the magnetic field magnitude generated by the circuit is linear up to 20% higher than the nominal magnetic field strength. Additionally, Figure 7b shows that up to 5.5 A each thruster is within 2% of the value expected based on inner coil current of 2 A until the curve begins to deviate from linearity. The deviation plotted here is the difference between the actual value at the given coil current and the value predicted based on proportionally scaling the magnetic field strength at 2 A for each thruster. Figure 7b shows each thrusters magnetic field peak is within 2% of all other thrusters for all measured inner coil currents. Given these small variations in magnitude and the fact that the magnet field maps in the channel were all quantitatively very similar, we ultimately determined that all thrusters passed this acceptance test.

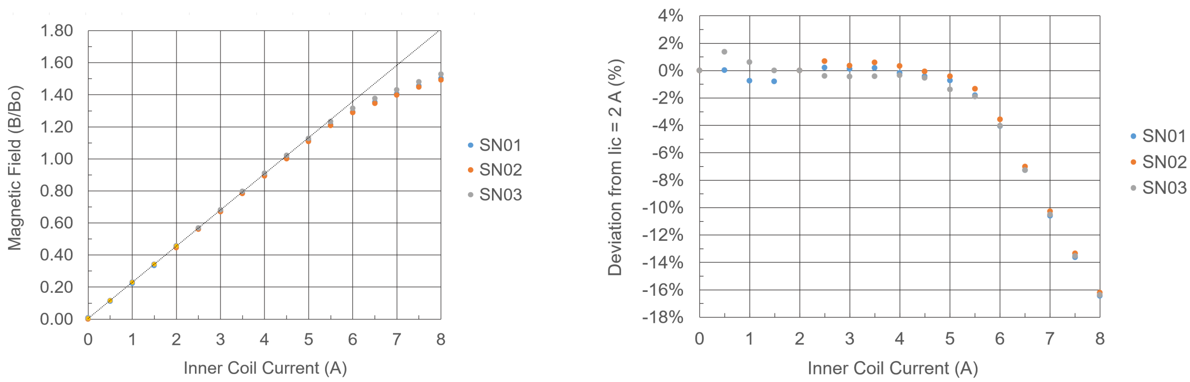

Figure 7: (a) Inner coil current versus relative magnetic field strength showing linearity in the circuit up to 20% above the nominal magnetic field setting for each thruster. (b) Deviation in expected magnetic field strength in percent based on a proportional scaling relative to inner coil current at two amps. Results show that each thruster is withing 2% of each other thruster and the circuit is linear until inner coil current is at 5.5 A.

IV. Performance Testing

We divided the performance tests between the two facilities available to us for this campaign. The stability maps and far-field maps were performed on all three thrusters at the University of Michigan's LVTF while we performed thrust measurements at JPL only on the thruster built for this facility, the SN03. We show in Table 1 the test matrix of operating conditions we examined at each test location.

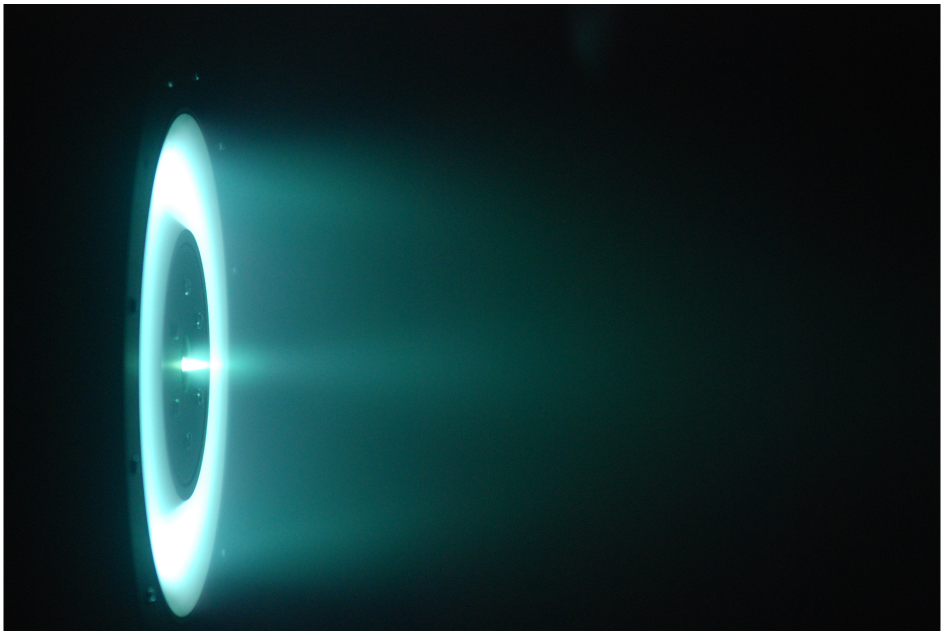

Figure 8: The H9 SN01 firing in the Large Vacuum Test Facility at the University of Michigan during initial performance testing.

A. Test Matrix

Table 1: Test Matrix at UM (left) and at JPL (right).

Test Matrix at the University of Michigan			
Test Point	Voltage [V]	Current [A]	Power [kW]
1	300	15	4.5
2	300	20	6
3	400	15	6
4	500	15	7.5
5	600	15	9
6	800	11.25	9

Test Matrix at the Jet Propulsion Laboratory				
Test Point	Voltage [V]	Current [A]	Power [kW]	$\frac{B}{B_o}$
1	300	15	4.5	0.78
2	300	15	4.5	1.00
3	300	20	6	0.78
4	300	20	6	1.00
5	400	15	6	0.89
6	400	15	6	1.00
7	500	15	7.5	1.00
8	600	15	9	1.00
9	800	11.25	9	1.00
10	800	11.25	9	1.11

We note that the use of two facilities does invite questions about the uniformity and interchangeability of results and test conditions. To address this potential concern, we recorded both the required mass flow rate for a constant power as well as the background pressure for the same operating conditions at both the University of Michigan and the Jet Propulsion Laboratory. As Figure 10 shows, the results indicate that at two different facilities of different pumping speed and size, the maximum deviation in background pressure between like conditions was 8.9%. Furthermore, even with the given deviation in background pressure, the maximum deviation in mass flow rate for constant power operation was 2.6%. These results indicate that operating conditions are repeatable from facility to facility as 2.6% is generally on the order of or less than the uncertainty for many of the measurements taken (e.g. generally about 1 percent for thrust and 2.4 percent for efficiency).

Figure 10: Comparison of anode mass flow rate and facility pressure for the SN03 firing at UM and at JPL.

Vd (V)	Id (A)	B/Bo	Anode Mass Flow Rate JPL (mg/s)	Anode Mass Flow Rate PEPL (mg/s)	**% Difference**	Pressure at PEPL (uTorr-Xe)	Pressure at JPL (uTorr-Xe)	**% Difference**
300	15	0.78	14.70	14.89	**1.3**	11.6	11.1	**4.5**
300	20	0.78	18.58	18.61	**0.2**	14.4	13.8	**4.3**
400	15	0.893333	15.02	15.42	**2.6**	12.3	11.3	**8.8**
500	15	1	15.27	15.67	**2.6**	12.3	11.6	**6.0**
600	15	1	15.46	15.35	**0.7**	12.5	11.9	**5.0**
800	11.25	1.106667	12.65	12.82	**1.3**	10.8	10.4	**3.8**

B. Indications of magnetic shielding

Throughout the testing campaigns, there were many qualitative indications that the magnetic shielding topography had been achieved. Figure 11 shows, for example, noticeable carbon deposition on the thruster discharge chamber after approximately 10 hours of firing. With an unshielded thruster, we would expect to see carbon deposition deep in the discharge chamber, but closer to the exit plane where erosion from beam interaction occurs, the rings should remain white. Figure 11 shows that carbon is coating the entirety of the discharge chamber and rings. This is the first qualitative indication of magnetic shielding.[2] As a second indication (Figure 9), we observed during operation that there was a zone of high light emission in the center of the channel, with decreased intensity near the walls to the point that the anode could be seen while the thruster was firing. This again is a qualitative indication of magnetic shielding as it indicates a cooler electron temperature at the discharge chamber boundary. This was previously noted for the H6MS shielded thruster in Ref. 2. Despite these qualitative indications, we do note here that these observations are necessary but not sufficient criteria to claim that the thrusters are shielded. However, since these qualitative indications are present, as well as the H9 following the same design philosophy of the H6MS and HERMeS, both of which have quantitative measurements of shielding, we are able to say that the thrusters are shielded.

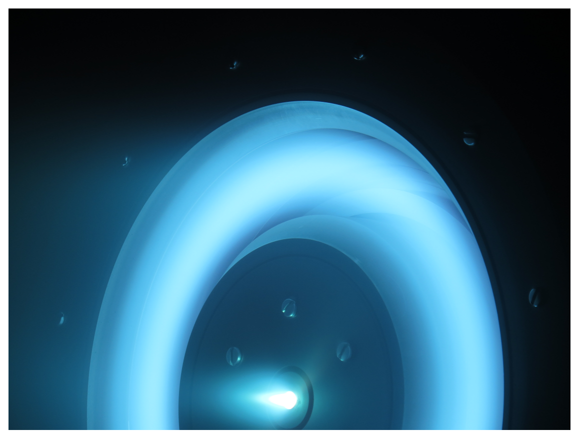

Figure 9: Zoomed in photo of the H9 SN03 discharge chamber during testing at JPL.

C. Thrust

Before taking thrust measurements at each operating condition, we first performed a magnetic field optimization. The details of this are discussed in Sec. IVD, but in brief, we parametrically varied the magnetic field intensity at each operating condition and monitored oscillations in the discharge current. We selected the magnetic field based on where these oscillations are minimized. With this in mind, we show in Fig. 12

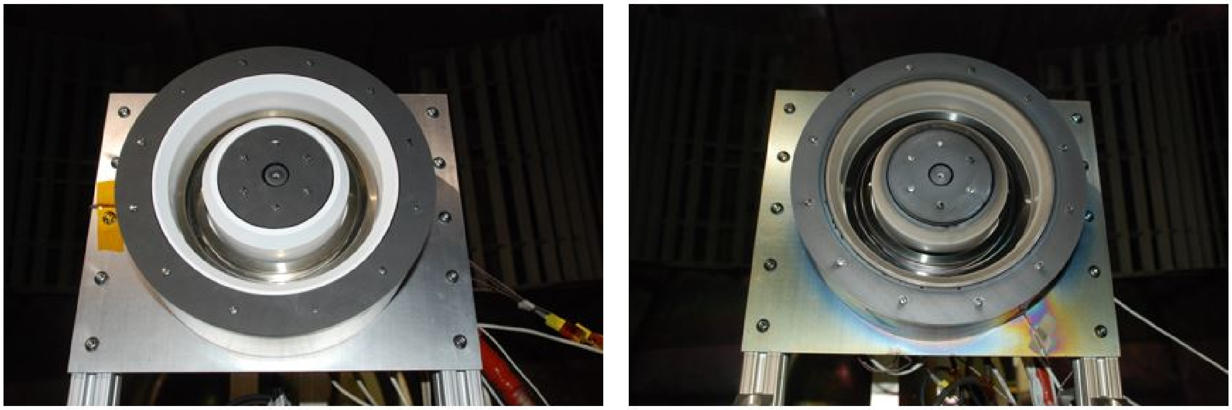

Figure 11: The H9 before firing (left) and after approximately 10 hours of firing (right) at the University of Michigan. Build up of carbon along the entirety of the discharge chamber walls is a qualitative indication of achieving a magnetic shielding topology.

the results of H9 SN03 thrust measurements from the campaign conducted at JPL. As would be expected, the thrust increases with current and discharge voltage: $T \propto I_d\sqrt{V_d}$. We also show in these figures for reference, the performance measurements of the H6MS at 300 V and 6 kW.[20] As can be seen, the H9 has almost the exact same performance at the same input value. This is to be expected because the thruster leverages many design features including major dimensions.

From these measurements, the flow rates, and input power, we similarly were able to determine the specific impulse $I_{sp} = \frac{T}{\dot{m}g}$ (Fig. 14) and total efficiency $\eta = \frac{T^2}{2\dot{m}P}$ (Fig 15). The figures indicate state-of-the-art performance with throttle-ability in the specific impulse from 1900 s to 2900 s all while maintaining total efficiency above 60%. Figure 13 shows the thrust-to-power for increasing discharge voltage. At constant current, the thrust-to-power decreases with increasing voltage as expected ($\frac{T}{P} \propto \frac{1}{\sqrt{V_d}}$) In turn, the I_{sp} of the thruster increases as seen in Figure 14. Finally, Figure 15 shows the H9 SN03 efficiency for all operating conditions. The thruster efficiency varies from 60% to 64% across all operating conditions. In general, the H9 performance is on par with other state-of-the-art magnetically shielded thrusters showing thrust-to-power up to 65 mN/kW, specific impulse up to 2950 seconds and efficiencies up to 64%. A full table of performance can be seen in the companion paper.[9] At the comparison point to the H6MS, with a relative magnetic field strength of 0.78, the H9 SN03 produced 385 mN of thrust at an efficiency of 61.6% and an I_{sp} 1974 seconds.

Finally, a operating point to operating point comparison between the H6MS[20, 24] and the H9 SN03 is made in Figure 16. The results show that the largest deviation in performance between the H6MS and the H9 is 3.6% and the large majority of results are within 2% of each. Considering the uncertainty on thrust and mass flow rate is 1% each, most of these point lie within uncertainty of each other.

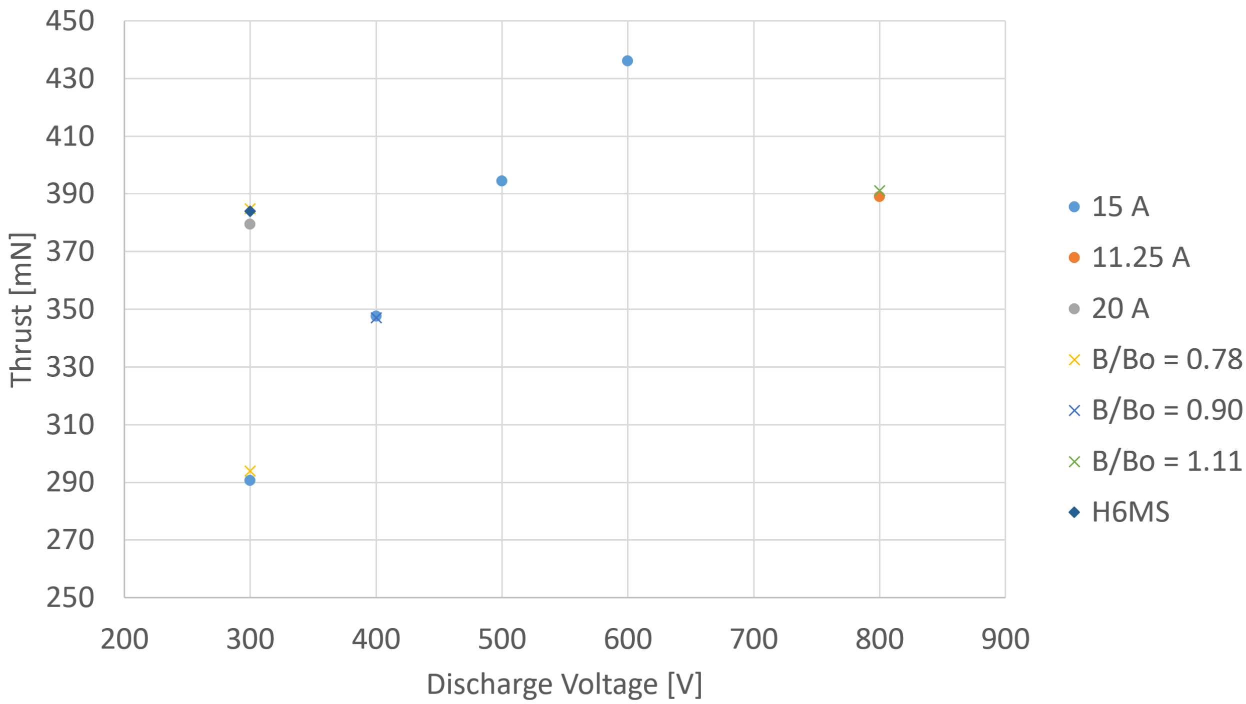

Figure 12: Thrust versus discharge voltage for the SN03. The H6MS at 300 V, 20 A is also present for reference.

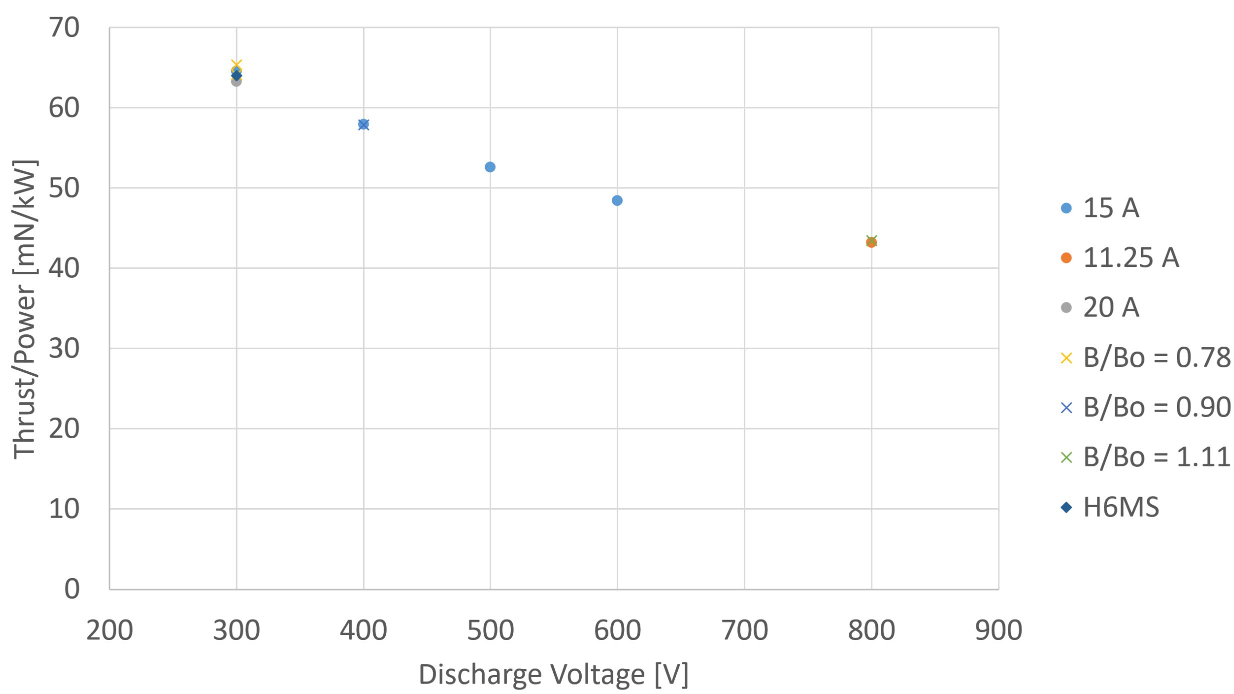

Figure 13: Thrust/power versus discharge voltage for the H9SN03.

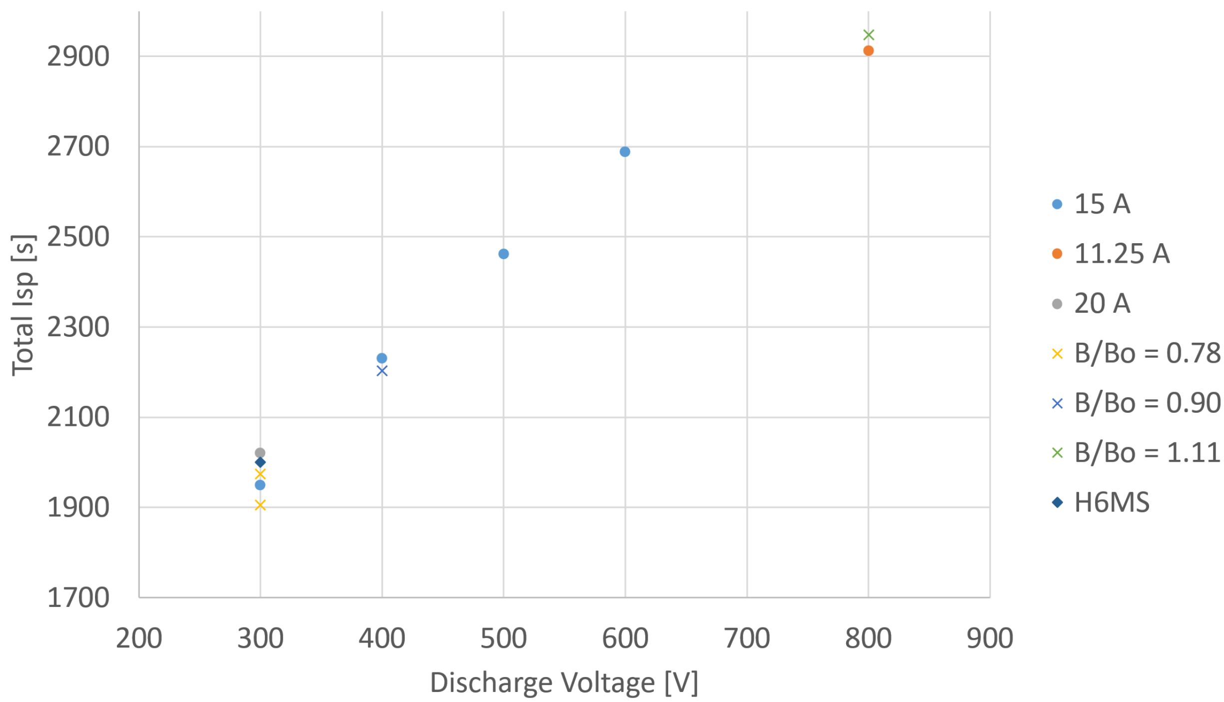

Figure 14: I_{sp} versus discharge voltage for the H9 SN03. The specific impulse of the H9SN03 maximizes at 2947 seconds.

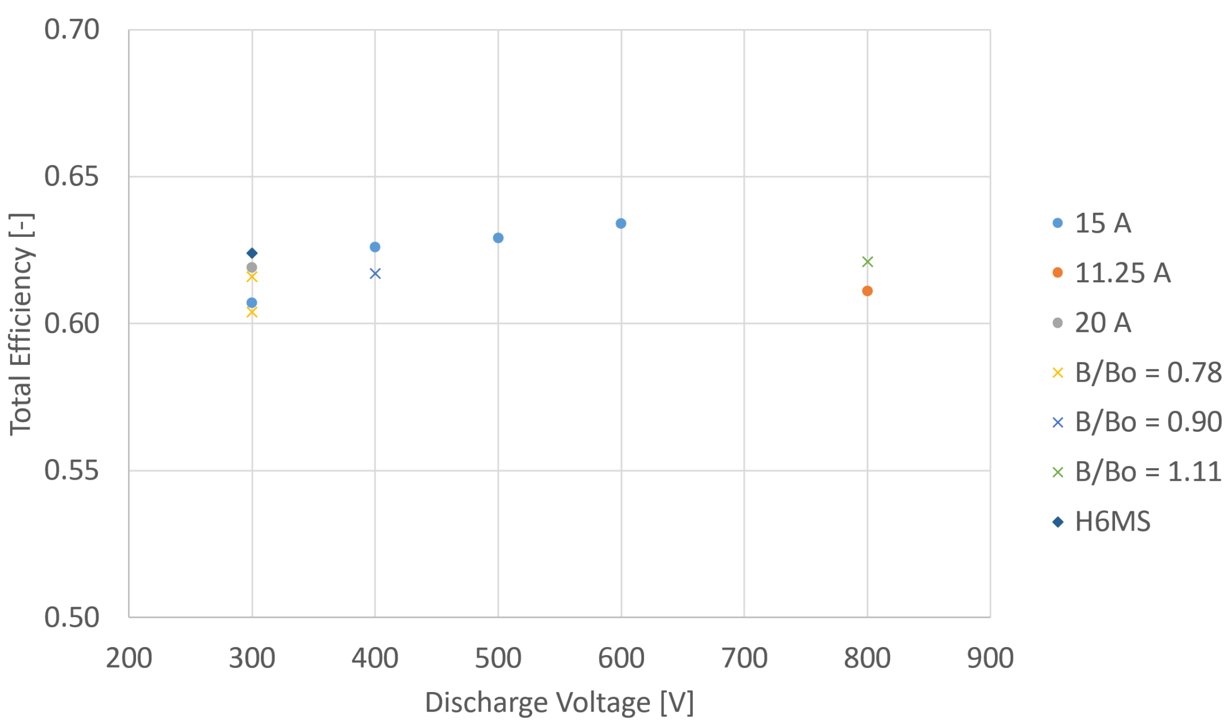

Figure 15: Thruster efficiency versus discharge voltage for the SN03. At all conditions the thruster performed greater than 60% and maximized at 63.4%.

Vd (V)	Id (A)	Thrust H9 (mN)	Thrust H6MS (mN)	% Difference	Total Isp H9 (s)	Total Isp H6MS (s)	% Difference	Total Eff H9	Total Eff H6MS	% Difference
300	15.0	294	294	0.0	1906	1910	-0.2	0.604	0.601	0.5
300	20.0	384	384	0.0	1974	2000	-1.3	0.616	0.624	-1.3
400	15.0	348	348	0.0	2231	2210	1.0	0.626	0.626	0.0
500.2	15.0	394.5	402	-1.9	2462	2470	-0.3	0.629	0.641	-1.9
600.2	15.0	436	447	-2.5	2688	2730	-1.5	0.634	0.658	-3.6
800.1	11.25	391.2	390	0.3	2947	3020	-2.4	0.621	0.636	-2.4

Figure 16: Comparison of the H6MS performance[20, 24] and H9SN03 performance at each operating conditions. For conditions where there are multiple H9 test points, the point with the highest thrust value was used for comparison.

D. Discharge current oscillations

Discharge current oscillations were measured with a Tektronix AC coupled clamp-on current probe at JPL and UM. The data during testing at JPL can be seen in Table 2 and Fig. 17. The table shows that at no point during the testing were the peak-to-peak oscillations greater than 80% the mean. There are two different frequencies at which the thruster tends to oscillate depending on the operating conditions: 10-20 kHz or 65-75 kHz. This behavior is similar to the behavior seen in the H6MS.[6] The thrusters appear to have a breathing mode at approximately 10-20 kHz, which is seen in most Hall thrusters. Additionally, in Figure 20, the breathing intensity is seen to increase with decreasing magnetic field as expected.[25]

Table 2: Oscillation Behavior for the H9SN03 during testing at JPL

Vd	Id	B/Bo	P2P/Id (%)	RMS/Id (%)	Freq (kHz)
300	15	0.78	42.1	5.1	12.2
300	15	1.00	32.5	4.6	9.2
300	20	0.78	57.6	7.7	12.2
300	20	1.00	33.2	5.0	76.3
400	15	0.89	61.9	6.0	15.3
400	15	1.00	70.4	8.2	18.3
500	15	1.00	65.6	12.3	67.1
600	15	1.00	75.7	15.3	64.1
800	11.25	1.00	73.2	11.1	70.2
800	11.25	1.11	79.6	12.1	73.2

During testing at the University of Michigan, we performed stability and magnetic field margin maps by sweeping the magnetic field magnitude from $0.67B_0$ to $1.4B_0$ and monitoring the discharge current oscillations. The average value of discharge current as well as the peak-to-peak (P2P) oscillation values of SN03 are shown in Figure 21 where we can see that the current oscillations only show incremental changes with magnetic field. There is a slight rise with lowering magnetic field, which is an indication that this region in parameter space may be the edge of the so-called global mode transition.[25] As we discussed briefly in Sec. IVC, we performed these maps at each operating condition and chose the magnetic field strength that minimized both oscillations and DC current before taking performance data.

With that said, Figure 21 is indicative of the oscillatory behavior of all the thrusters. It is interesting to note that in the 400 V condition the oscillations increase and then decrease with decreasing magnetic field Figures 18, 19, and 20 compare the DC current and peak-to-peak oscillations of all three thrusters at three operating conditions. Results show that all three thruster have very similar oscillation behavior at each operating condition. This is additional proof of uniformity in construction and operation.

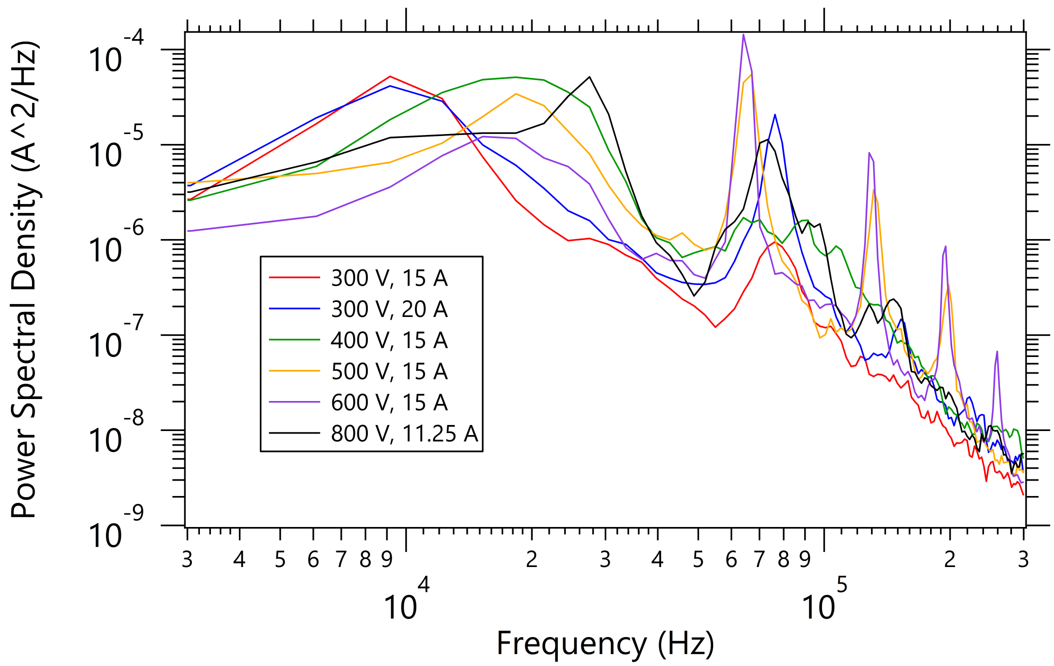

Figure 17: Power spectral density for all test points with nominal magnetic fields from H9SN03 testing at JPL.

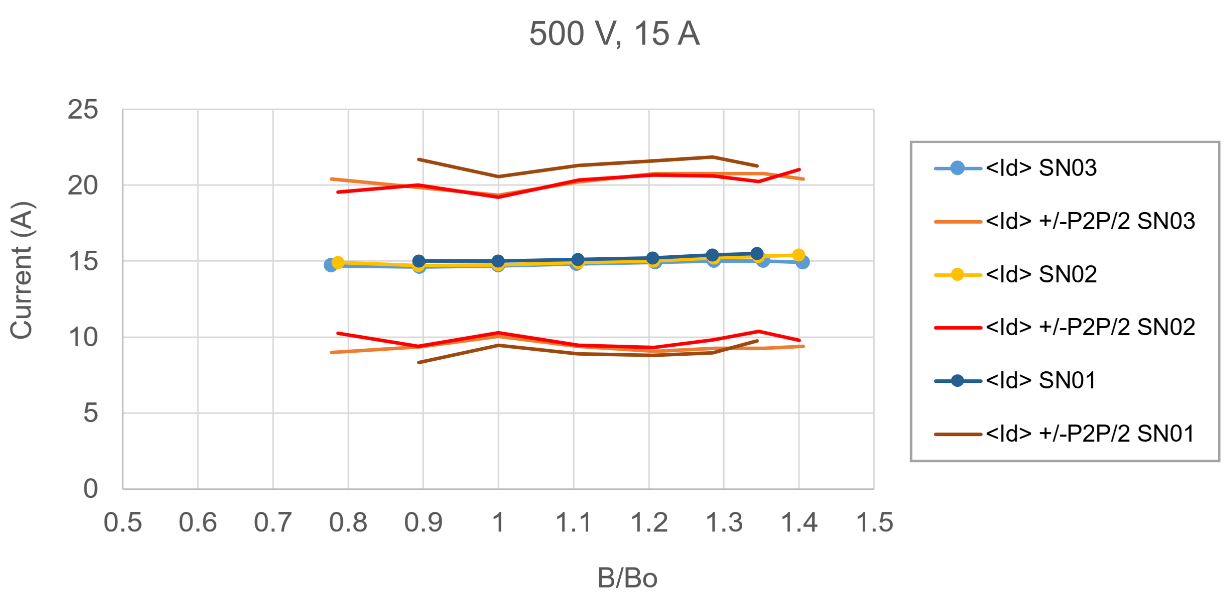

Figure 18: Comparison of the mean discharge current and P2P oscillations versus magnetic field strength for each thruster during testing at UM for the 500 V, 15 A condition.

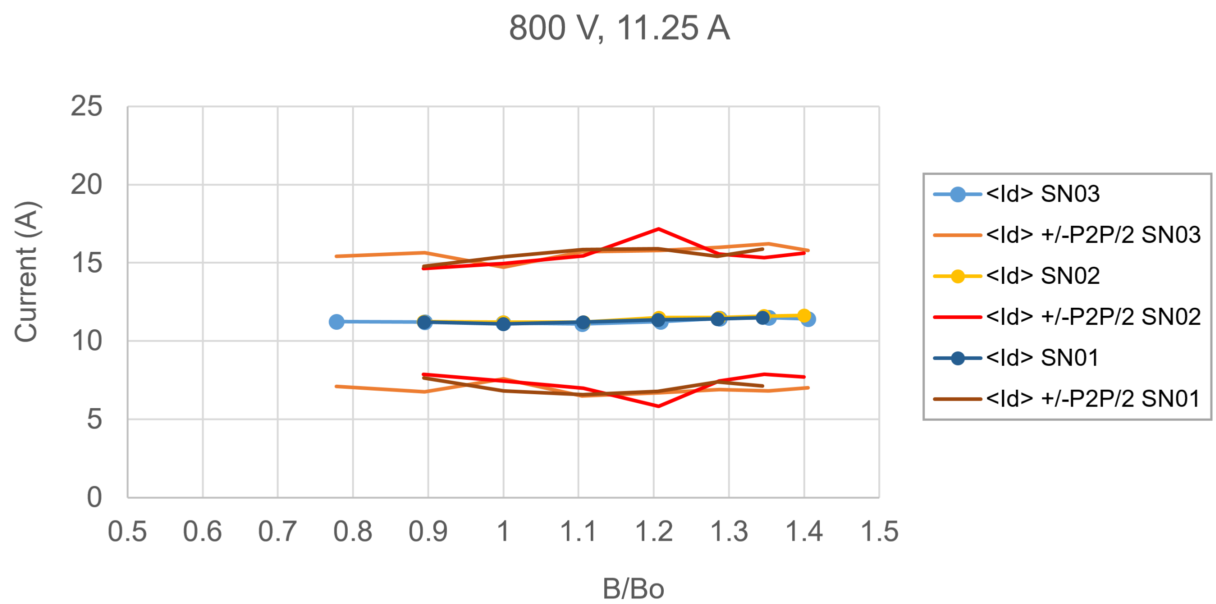

Figure 19: Comparison of the mean discharge current and P2P oscillations versus magnetic field strength for each thruster during testing at UM for the 800 V, 11.25 A condition.

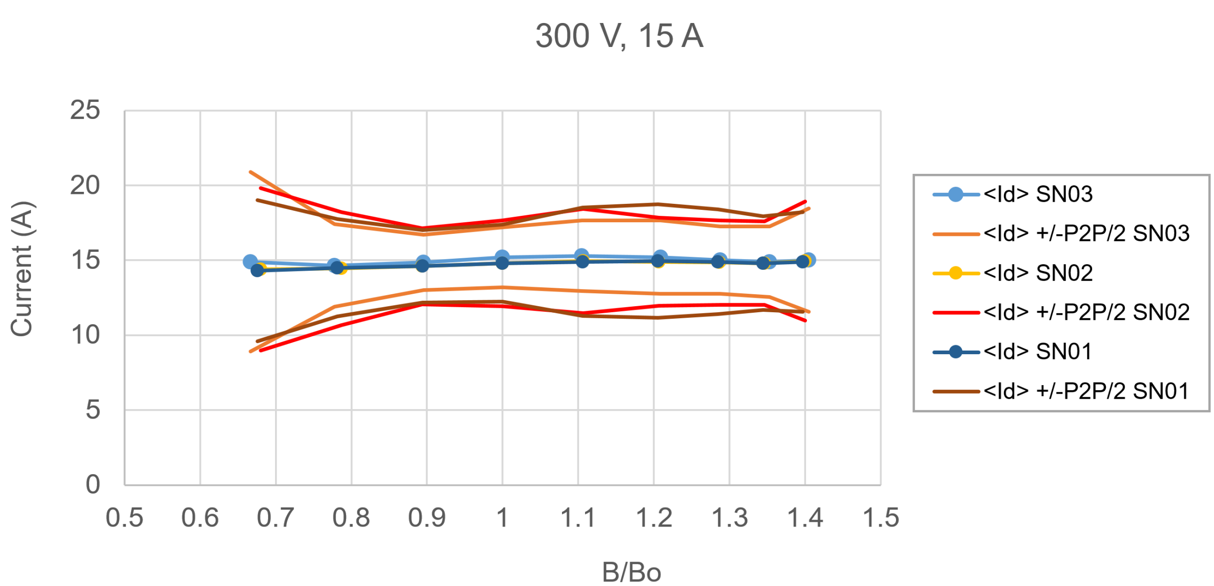

Figure 20: Comparison of the mean discharge current and P2P oscillations versus magnetic field strength for each thruster during testing at UM for the 300 V, 15 A condition.

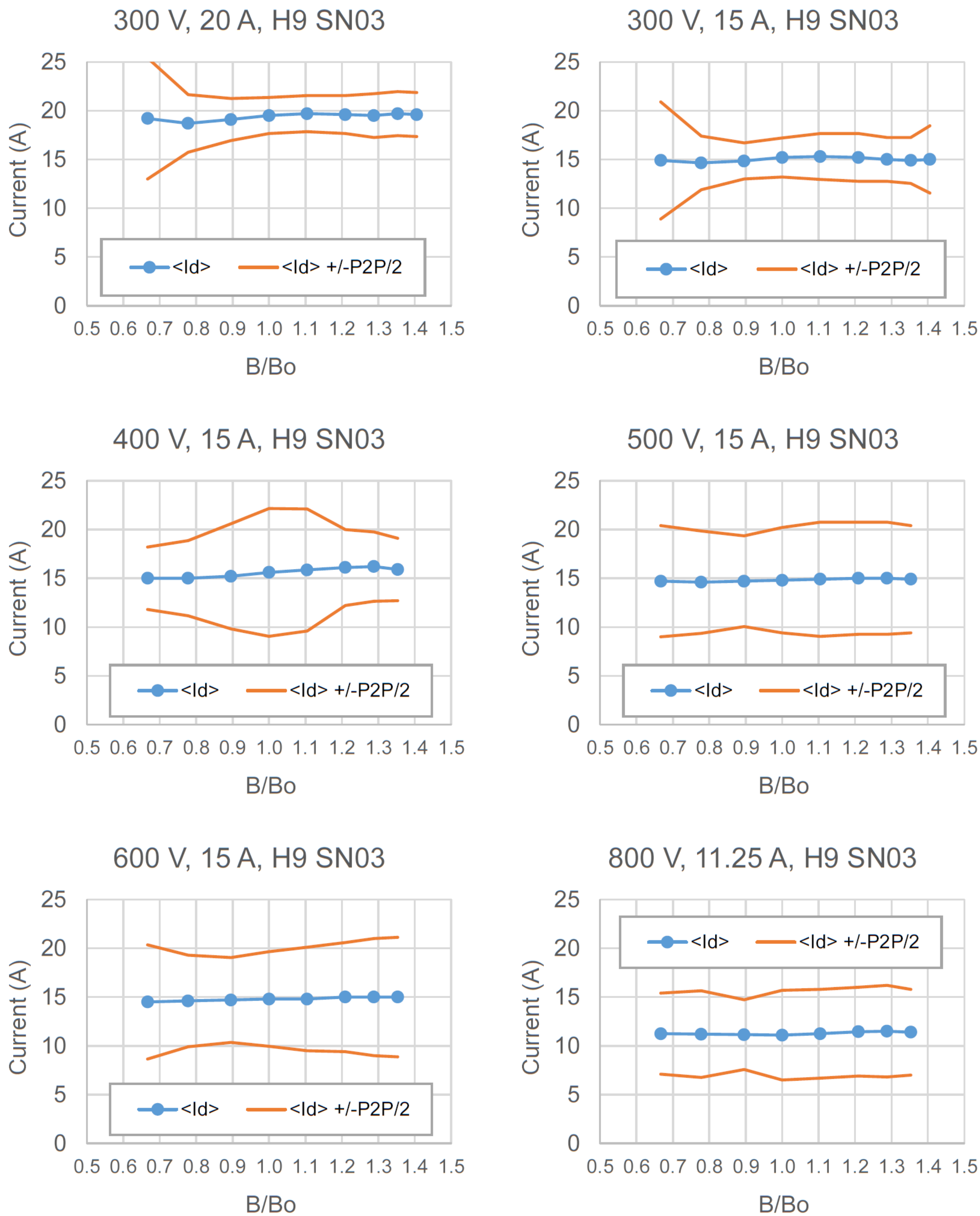

Figure 21: Magnetic field sweeps for each operating condition at UM for SN03. The plots show mean discharge current and P2P for varying magnetic field strength. These plots are representative of each thruster.

E. Ion Current Density

Using a Faraday probe, we took ion current density measurements at the University of Michigan to assess thruster symmetry and similarity between thrusters. Faraday probe traces for each thruster at constant 15 A throttling can been seen in Figure 22. The 600 V condition for SN01 data was corrupted therefore, it is not shown here. Qualitatively, all thrusters have good symmetry at each operating condition. The slight difference in peak height on some of the traces seen in Figure 22 can likely be attributed to differences in flow uniformity. Overall, however, the difference are all less than 10% which was the allowable variation in anode flow uniformity. Figure 23 shows the traces of each thruster laid on top of each other for three

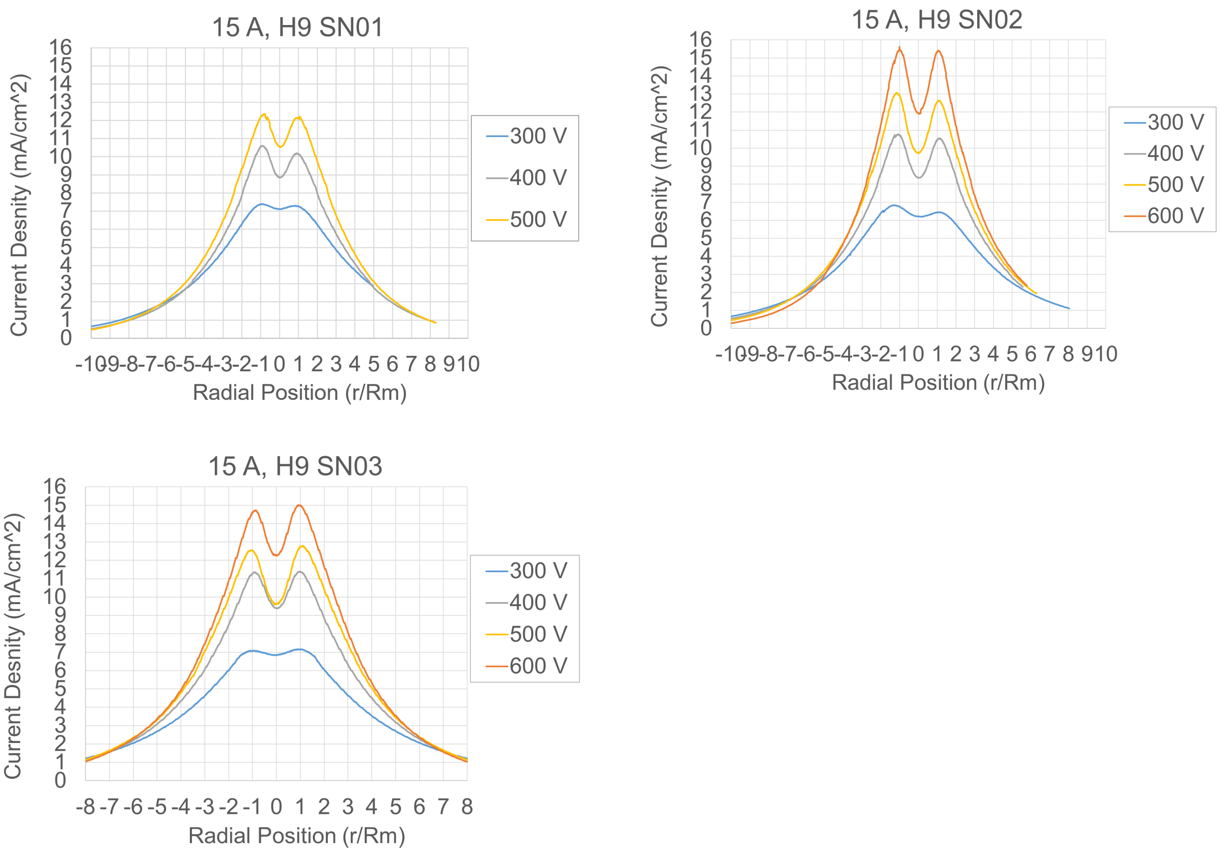

Figure 22: Faraday probe sweeps for each 15 A condition for each thruster. Good symmetry is seen in the traces for each thruster.

sample operating conditions. All thrusters show very good agreement with each other. There are very slight differences as expected. Some difference can be attributed to using a different Faraday probe for SN03 versus SN01 and SN02. This was due to Probe 1 having a probe failure during SN01 and SN02 testing. Finally, Figure 24 shows an example trace at 800 V, 9 kW for SN02. This trace, combined with the other traces, indicates that the thrusters are performing as expected across the nominal operating envelope.

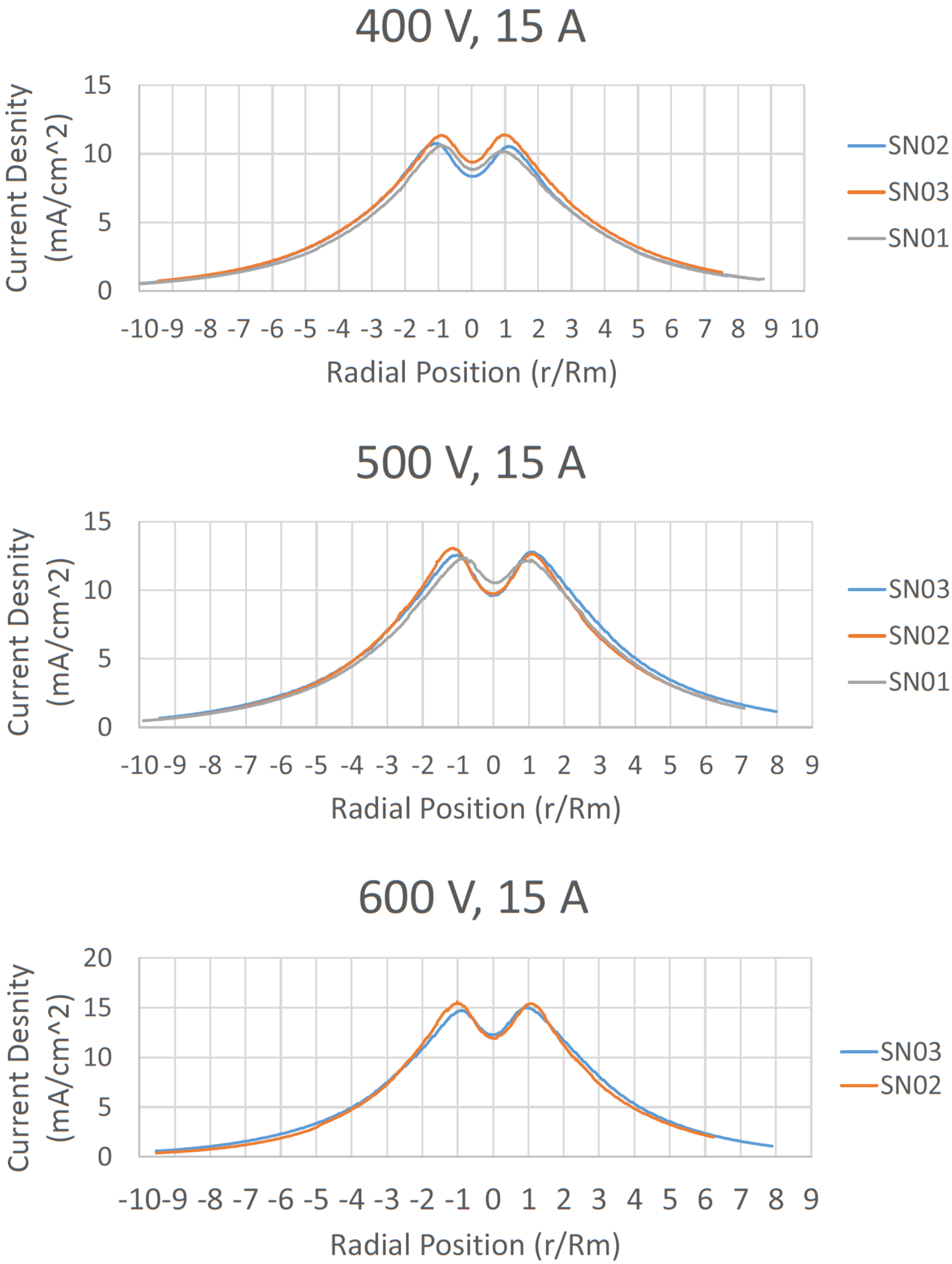

Figure 23: Comparison of ion current density traces for each thruster at the 300, 400 and 500 V conditions.

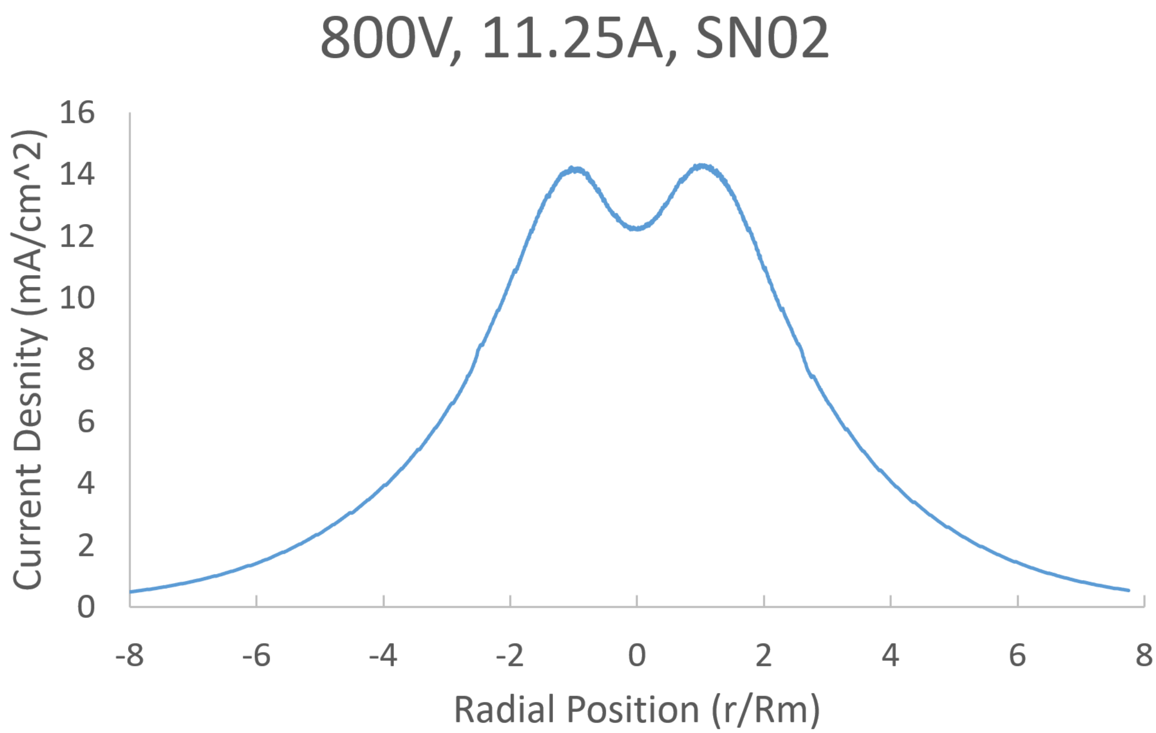

Figure 24: Ion current density trace at 800 V, 9 kW for SN02 taken at UM. This trace is representative of all thrusters showing a uniform plume at high voltage.

V. Conclusion

Three H9 Hall thrusters were tested to assess stability and performance. All thrusters passed initial acceptance testing with maximum anode flow uniformity deviations ranging from 4.05-9.23% at low flow and 3.35-6.46% at high flow. The thrusters all showed 20% margin on nominal magnetic field strength before saturation onset and were within 2% of each other for inner coil current vs magnetic field strength. H9 SN03 was tested at both the University of Michigan and the Jet Propulsion Laboratory with the maximum difference in anode flow rate for a given condition at 2.6% showing that thruster operation is repeatable from facility to facility. The thruster produced 384 mN of thrust and 1970 seconds of specific impulse at 300V, 6 kW which is within 1.3% of H6MS at the same condition. At 800 V, 9 kW, the thruster produced 2950 seconds of I_{sp}. The thruster showed stability over a range of magnetic field strength with oscillation strength never exceeding the DC discharge current. Faraday probe measurements show plume symmetry within 10% peak height and thruster to thruster agreement. The H9 thrusters also proved to have similar performance as other state-of-the-art magnetically shielded Hall thrusters. Overall, the H9 thrusters have shown to be able to be tested at multiple facilities, have good stability and agreement with each other, and now provide a platform for continued physics research at high discharge voltages.

Acknowledgments

Portions of the research described in this paper were carried out at the Jet Propulsion Laboratory, California Institute of Technology, under a contract with the National Aeronautics and Space Administration. The authors would like to acknowledge funding provided by the NASA Space Technology Research Fellowship grant number NNX15AQ43H. The authors would also like to thank Ray Swindlehurst at JPL for all his help during thruster construction and testing as well as the members of the Plasmadynamics and Electric Propulsion Laboratory for all their support during initial testing.

References

[1]Mikellides, I. G., Katz, I., Hofer, R. R., and Goebel, D. M., "Magnetic shielding of a laboratory Hall thruster. I. Theory and validation," *Journal of Applied Physics*, Vol. 115, No. 4, 2014.

[2]Hofer, R. R., Goebel, D. M., Mikellides, I. G., and Katz, I., "Magnetic shielding of a laboratory Hall thruster. II. Experiments," *Journal of Applied Physics*, Vol. 115, No. 4, 2014.

[3]De Grys, K., Mathers, A., Welander, B., and Khayms, V., "Demonstration of 10,400 Hours of Operation on 4.5 kW Qualification Model Hall Thruster," *AIAA paper*, Vol. 6698, 2010, pp. 2010.

[4]Mikellides, I. G., Katz, I., Hofer, R. R., Goebel, D. M., De Grys, K., and Mathers, A., "Magnetic shielding of the channel walls in a Hall plasma accelerator," *Physics of Plasmas*, Vol. 18, No. 3, 2011, pp. 033501.

[5]Mikellides, I. G. and Katz, I., "Numerical simulations of Hall-effect plasma accelerators on a magnetic-field-aligned mesh," *Physical Review E*, Vol. 86, No. 4, 2012, pp. 046703.

[6]Jorns, B. A. and Hofer, R. R., "Plasma oscillations in a 6-kW magnetically shielded Hall thruster," *Physics of Plasmas*, Vol. 21, No. 5, 2014, pp. 053512.

[7]Hofer, R., Kamhawi, H., Herman, D., Polk, J., Snyder, J. S., Mikellides, I., Huang, W., Myers, J., Yim, J., Williams, G., et al., "Development approach and status of the 12.5 kW HERMeS Hall thruster for the solar electric propulsion technology demonstration mission," *34th International Electric Propulsion Conference*, 2015, pp. 4–10.

[8]Hofer, R., Kamhawi, H., Mikellides, I., Herman, D., Polk, J., Huang, W., Yim, J., Myers, J., and Shastry, R., "Design Methodology and Scaling of the 12.5 kW HERMeS Hall Thruster for the Solar Electric Propulsion Technology Demonstration Mission," *62nd JANNAF Propulsion Meeting*, 2015.

[9]Hofer, R. R., Cusson, S. E., and Lobbia, R. B., "The H9 Magnetically Shielded Hall Thruster," *35th International Electric Propulsion Conference*, 2017.

[10]Hofer, R., Goebel, D., and Watkins, R., "Compact LaB6 Hollow Cathode for the## Hall Thruster," *54th JANNAF Propulsion Meeting*, pp. 14–17.

[11]Hofer, R., Polk, J., Sekerak, M., Mikellides, I., Kamhawi, H., Sarver-Verhey, T. R., Herman, D. A., and Williams, G., "The 12.5 kW Hall Effect Rocket with Magnetic Shielding (HERMeS) for the Asteroid Redirect Robotic Mission," *52nd AIAA/SAE/ASEE Joint Propulsion Conference*, 2016, p. 4825.

[12]Katz, I., Lopez Ortega, A., Goebel, D., Sekerak, M., Hofer, R., Jorns, B., and Brophy, J., "Effect of Solar Array Plume Interactions on Hall Thruster Cathode Common Potentials," *14th Spacecraft Charging Technology Conference*, 2016.

[13]Hofer, R. R., Jorns, B. A., Brophy, J. R., , and Katz, I., "Hall Effect Thruster Electrical Configuration," Tech. rep., California Institute of Technology, USPTO patent application submitted, March 30, 2017.

[14]Florenz, R., *The X3 100-kW Class Nested-Channel Hall Thruster: Motivation, Implementation, and Initial Performance*, Ph.D. thesis, University of Michigan, Ann Arbor, MI, 2014.

[15]Hall, S. J., Cusson, S. E., and Gallimore, A. D., "30-kW Performance of a 100-kW Class Nested-channel Hall Thruster," *34th International Electric Propulsion Conference*, Kobe, Japan, 2015.

[16]Goebel, D. M., Jameson, K. K., and Hofer, R. R., "Hall thruster cathode flow impact on coupling voltage and cathode life," *Journal of Propulsion and Power*, Vol. 28, No. 2, 2012, pp. 355.

[17]Hofer, R. R., Johnson, L. K., Goebel, D. M., and Wirz, R. E., "Effects of internally mounted cathodes on Hall thruster plume properties," *IEEE Transactions on Plasma Science*, Vol. 36, No. 5, 2008, pp. 2004–2014.

[18]Randolph, T. M. and Polk, J. E., "An overview of the nuclear electric xenon ion system (NEXIS) activity," *AIAA Paper 2004-5909*, 2004.

[19]Hofer, R. R., Goebel, D. M., Snyder, J. S., and Sandler, I., "BPT-4000 hall thruster extended power throttling range characterization for NASA science missions," *31st International Electric Propulsion Conference, IEPC-2009-085, Ann Arbor, MI*, 2009.

[20]Hofer, R. R., Goebel, D. M., Mikellides, I. G., and Katz, I., "Design of a laboratory Hall thruster with magnetically shielded channel walls, phase II: Experiments," *AIAA paper*, Vol. 3788, 2012, pp. 2012.

[21]Hofer, R. R. and Anderson, J. R., "Finite Pressure Effects in Magnetically Shielded Hall Thrusters," _ *50th AIAA/ASME/SAE/ASEE Joint Propulsion Conference and Exhibit* _, 2014.

[22]Brown, D. L. and Gallimore, A. D., "Evaluation of ion collection area in Faraday probes," *Review of Scientific Instruments*, Vol. 81, No. 6, 2010.

[23]de Grys, K., Meckel, N., Callis, G., Greisen, D., Hoskins, A., King, D., Wilson, F., Werthman, L., and Khayms, V., "Development and testing of a 4500 watt flight type Hall thruster and cathode," *IEPC Paper*, 2001, pp. 01–011.

[24]Hofer, R., Jorns, B., Polk, J., Mikellides, I., and Snyder, J., "Wear test of a magnetically shielded Hall thruster at 3000 seconds specific impulse," *33rd International Electric Propulsion Conference*, 2013, pp. 1–24.

[25]Sekerak, M. J., *Plasma oscillations and operational modes in Hall effect thrusters*, Ph.D. thesis, University of Michigan, 2014.